

Original Research

Spatiotemporal Variations and Source of PM_{2.5} in the Sichuan Basin at Nanchong City, China

Yi-fan Qian^{1,2#}, Jie Xia^{2#o}, Dan-yu Li², Xiong Lei², Shi-dong Yu²,
Yun-xiang Li^{1*}, Qiu-mei Quan^{1**}

¹College of Environmental Science and Engineering, China West Normal University,
Nanchong 637009, Sichuan, China

²Nanchong Ecological and Environmental Monitoring Central Station of Sichuan Province,
Nanchong 637000, Sichuan, China

Received: 8 June 2024

Accepted: 9 September 2024

Abstract

To evaluate the pollution level, spatial and temporal variations and sources of fine particulate matter (PM_{2.5}) in Nanchong, a city in the Sichuan Basin, China, the trace element concentrations in PM_{2.5} were measured. The sources of PM_{2.5} were analyzed by the potential source contribution function (PSCF), enrichment factor (EF), and principal component analysis (PCA) methods from December 2014 to April 2016. The results showed that the mean concentrations of PM_{2.5} and the analyzed trace elements at the urban sites during the sampling periods were 58.89-63.03 μg m⁻³ and 2.81-3.43 μg m⁻³, respectively, and that those at the rural site were 60.13±4.28 μg m⁻³ and 2.55 μg m⁻³, respectively. There were no significant differences in the mean concentrations of PM_{2.5} or the analyzed trace elements between the urban area and the rural area. The seasonal variations in PM_{2.5} and the analyzed trace elements in the urban and rural areas were similar, with the order summer<spring<fall<winter. The PSCF analysis showed that the PM_{2.5} in the urban area of Nanchong City mainly originated from surrounding areas. The crustal elements K, Ca, Al, Na, Fe, Mg, and Ti were the dominant metals in the urban and rural areas of Nanchong, accounting for more than 93% of the total concentration of the analyzed trace elements. The EF of K was close to 20, indicating that it was derived mainly from anthropogenic sources. The EFs of Ca, Al, Na, Fe, Mg, and Ti were less than 10, indicating that these elements were derived mainly from natural sources. In contrast, although the concentrations of the trace elements Cu, Zn, As, Cd, Se, Ni, Pb, Ba, and Cr were relatively low, the EFs of each of these elements were much higher than 20, suggesting that these elements were mainly derived from anthropogenic sources. The EF and PCA results showed that the PM_{2.5} in Nanchong City mainly originates from natural sources, such as soil dust, and anthropogenic sources, such as biomass burning, construction dust, vehicular emissions, fireworks burning, etc.

Keywords: crustal elements, fine particulate matter, enrichment factor, principal component analysis, Nanchong City

#equal contribution

o0000-0001-9727-1445

*e-mail: yx_li@cwnu.edu.cn;

**e-mail: meimeiq@163.com

Introduction

In the past three decades, rapid economic development, urbanization, industrialization, and population agglomeration caused by the siphoning effect of cities in China have caused serious atmospheric pollution [1-8]. When the new Ambient Air Quality Standard (GB 3095-2012) replaced GB 3095-1996 and was gradually implemented in China in 2013 [9], most regions and cities with excessively poor ambient air quality were affected by fine particulate matter ($PM_{2.5}$, particulate matter with an aerodynamic diameter less than $2.5 \mu m$). Statistical assessments show that, in 2013, only 4.1% of the 74 important cities in China implemented new ambient air quality standards up to the $PM_{2.5}$ standard [10]. After nearly ten years of continuous effort by governments at all levels, many experts and scholars, and people worldwide, $PM_{2.5}$ pollution has been greatly alleviated, and only 25.4% of 339 cities in China had $PM_{2.5}$ concentrations exceeding the national standard in 2022 [11]. Overtime, $PM_{2.5}$ pollution, as the most important type of atmospheric pollution, has gradually become a public health concern and has become a research focus of scholars and experts because of its complex composition, wide range of pollution sources, influencing factors that vary from place to place, and great harm to human health [2, 4-5, 12-20].

Because the particle size of $PM_{2.5}$ is small, it can float in the air for a long time. In contrast, $PM_{2.5}$ has a large specific surface area and strong activity, and its surface can adsorb many carbonaceous components (sometimes called carbonaceous aerosols), water-soluble ions, and chemical elements [17, 21], which can then be carried into the human body through the respiratory tract and cause great harm to the human body, resulting in widespread scientific attention [19, 22]. $PM_{2.5}$ mainly originates from natural sources (such as soil dust, [5, 23]) and anthropogenic sources (such as biomass burning, vehicle exhaust, firework burning, and construction dust, [5, 23-25]). In the atmosphere, once adsorbed to $PM_{2.5}$, elements are less likely to react with other substances, so they can remain adsorbed on the surface of $PM_{2.5}$ for a long time. The contribution of each element to $PM_{2.5}$ varies with different pollution sources, so the source of pollutants can be analyzed by identifying the characteristic elements in $PM_{2.5}$. In the past, many experts and scholars have carried out many studies on the types, concentration levels, and sources of elements in $PM_{2.5}$ and analyzed the sources of $PM_{2.5}$ using models such as positive matrix factorization (PMF), chemical mass balance (CMB), and principal component analysis (PCA) [21, 25-26]. However, China has a vast territory, variable terrain, and different levels of economic development, and the developed regions (such as the Beijing–Tianjin–Hebei region [5, 19, 23, 27-29], the Yangtze River Delta region [5, 19, 23, 30-31], the Pearl River Delta region [5, 19, 23], etc.) and megacities [5, 32-40]) have attracted more attention than underdeveloped regions and smaller cities.

Nanchong City is a typical basin city, located in the northeastern Sichuan Basin and is the second most populous city in Sichuan Province. It is a typical agricultural city with fast development and a low level of industrialization. Its terrain slopes from north to south, with elevations between 888.8 and 256 meters. The urban area of the city is located in southern Nanchong City, with low elevations and extremely poor meteorological diffusion conditions for pollutants. The purpose of this study was to explore the pollution level, spatial and temporal variations, and sources of $PM_{2.5}$ and elements in the urban and rural areas of Nanchong City to compensate for the shortage of domestic research on the sources and prevention of $PM_{2.5}$ pollution in urban ambient air in the basin. The results of our study could provide insightful information and a scientific basis for the prevention and control of air pollution in basin cities and other types of Chinese cities in the future. The major objectives were as follows: (1) to determine the characteristics and sources of $PM_{2.5}$, (2) to analyze the seasonal variations in $PM_{2.5}$ in urban areas and rural areas, (3) to determine the degree of element enrichment in $PM_{2.5}$, and (4) to determine the sources of elements in $PM_{2.5}$.

Materials and Methods

Study Area

Nanchong City ($30^{\circ}35'31''N$, $105^{\circ}27'106''E$, 256-889 masl) is in the northeastern Sichuan Basin and in the midstream section of the Jialing River (Fig. 1a-b). This city has a mid-subtropical humid monsoon climate with four distinct seasons and is famous throughout the country for its poor meteorological diffusion conditions for pollutants, notably its breezy, damp, rainy, and foggy conditions. The landform type is mainly hilly, and the terrain slopes from north to south [41]. The urban area of Nanchong City is in the southern region and is at low elevations, i.e., approximately 300 meters (Fig. 1c). There are three districts in the main urban area of Nanchong, namely, Shunqing (SQ), Gaoping (GP), and Jialing (JL), with populations of more than 1.7 million and an area of approximately 170 km². In this study, one site was selected for $PM_{2.5}$ sample collection in each of the three districts and in a rural area (the rural site is in Guihua Township (GH)) located approximately 25 Kilometers from the urban area in the dominant upwind direction. The sampling site at SQ was situated on the rooftop (approximately 27 m above the ground) of the Nanchong Housing and Urban-Rural Development Bureau office building; at GP, it was situated on the rooftop (approximately 23 m above the ground) of the Gaoping Ecological and Environmental Bureau of Nanchong City office building; and at JL, it was situated on the rooftop (approximately 30 m above the ground) of the Jialing District People's Government's office building. The SQ, GP, and JL sampling sites were located

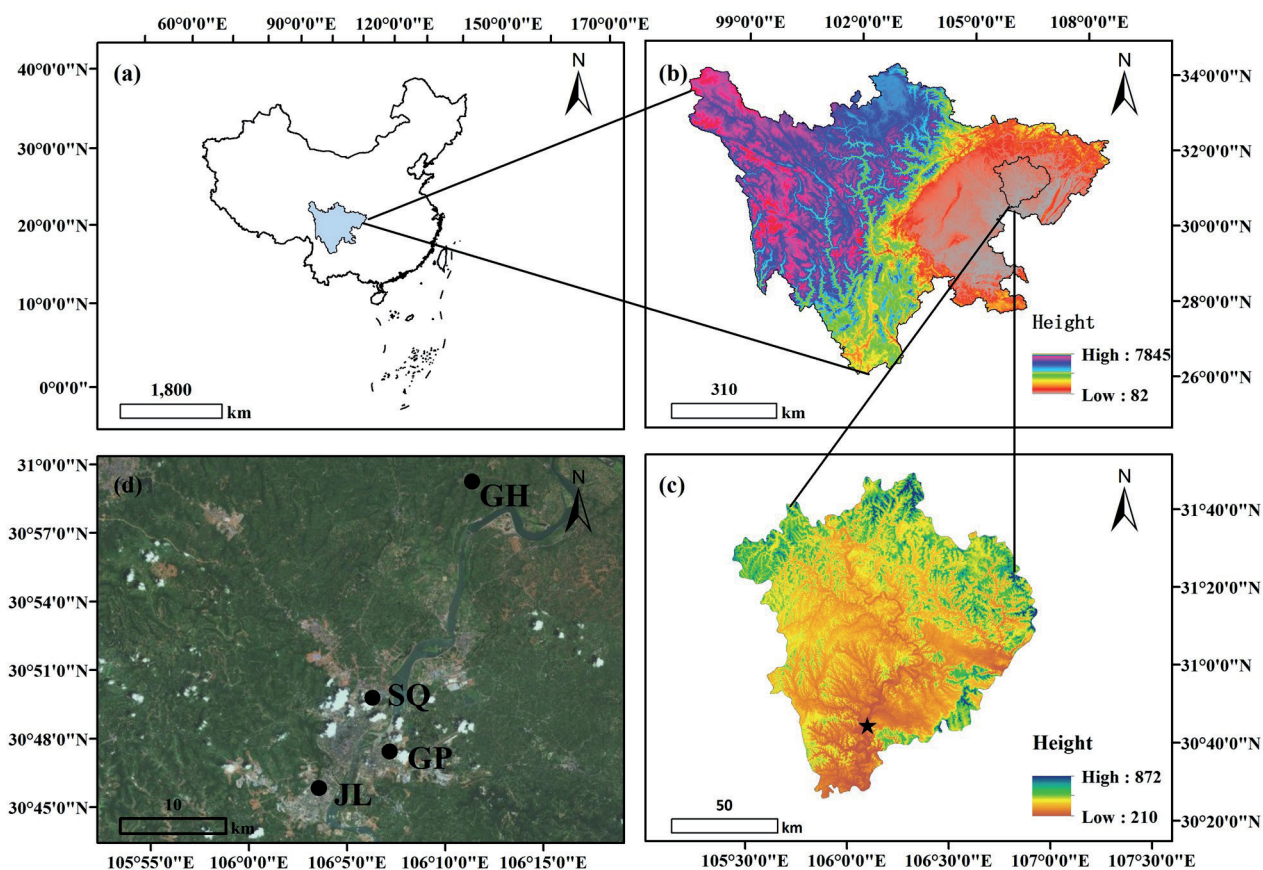


Fig. 1. a) The location of Sichuan Province in the southwest of China. b) The topography of the Sichuan Basin and the location of Nanchong in the northeastern Sichuan Basin. c) The topography of Nanchong. d) The Shunqing (SQ), Gaoping (GP), Jialing (JL), and Guihua (GH) sampling sites in Nanchong.

in mixed educational, commercial, traffic, and residential areas, and no obvious industrial pollution sources were detected within 3 km. Thus, the SQ, GP, and JL sampling sites can represent the urban environments of the Shunqing District, Gaoping District, and Jialing District, respectively. The sampling site at GH was located on the rooftop of the Guihua Township People's Government office building (approximately 8 m above the ground); this sampling site was surrounded by woodland, farmland, and villages without industrial pollution sources. The $PM_{2.5}$ sampling sites are shown in Fig. 1d).

Sampling and Analysis

The $PM_{2.5}$ samples were collected synchronously at the SQ, GP, JL, and GH sampling sites from December 22, 2014, to April 27, 2016. The $PM_{2.5}$ samples were collected every six days with a four-channel sampler (each channel maintained a flow rate of 16.7 L min^{-1}) made by Tianhong Instrument Co., Ltd., of China (TH-16A), and the duration of each sampling was 24 hours (from 10:00 a.m. to 10:00 a.m. of the next day). A total of 86, 65, 74, and 89 samples were collected at SQ, GP, JL, and GH, respectively (Table S1). The $PM_{2.5}$ samples were collected on Teflon and quartz

filters. The procedures for membrane replacement and sample storage were conducted following the Technical Guidelines for Source Analysis and Monitoring of Atmospheric Particulates (Trial) [42].

The Teflon filters were weighed at least three times with an electronic balance made by Mettler-Toledo Intl., Inc., USA (AX105 DeltaRange) after being balanced for 24 h in a super-clean environment at a constant temperature ($20 \pm 1^\circ\text{C}$) and relative humidity ($40\% \pm 3\%$). The $PM_{2.5}$ concentration was obtained by dividing the mass difference of the Teflon filter before and after sampling by the sampled air volume.

The Teflon filters were nitrated in a solution of 3 mL HNO_3 (65%), 1 mL HCl (38%), and 0.2 mL HF (48%) at 175°C for 1 hour. The nitrification liquids were cooled to room temperature and diluted to 100 mL with ultrapure water, and the elemental concentrations (Na, Mg, Al, Ca, Fe, K, Mn, Cu, Zn, As, Ti, Cd, Se, Ni, V, Pb, Co, Ba, and Cr) in the solutions were analyzed via inductively coupled plasma-mass spectrometry (Agilent 7500c, Agilent Technologies Co., Ltd., USA).

The hourly concentrations of $PM_{2.5}$ and PM_{10} were used to calculate and evaluate the proportion of $PM_{2.5}$ in PM_{10} . The tracked aerological data for air masses (such as pressure and wind speed) for backward trajectory analysis were obtained from the Air Resource

Table S1. The numbers of samples of PM_{2.5} at SQ, GP, JL, and GH.

Sampling sites	Spring	Summer	Autumn	Winter	Total
SQ	24	15	14	33	86
GP	19	15	13	18	65
JL	17	16	8	33	74
GH	20	15	13	41	89

Laboratory, National Oceanic and Atmospheric Administration (<http://www.arl.noaa.gov/>). The hourly concentrations of PM_{2.5} and the tracked aerological data were used to calculate the potential source contribution function (PSCF).

Data Processing and Statistical Analysis

Potential Source Contribution Function (PSCF)

In this study, Metewoinfo software (download website: <http://www.meteothinker.com>) was used to analyze the 24-h backward trajectories of 500-m-high air masses in the urban area of Nanchong (30.80 N, 106.08 E, 500 m AGL) [43]. Then, the PSCF model in MetewoFo software, based on the results of backward trajectory analysis, was used to identify the potential source regions of PM_{2.5}.

PSCF analysis relies on the conditional probability function as the basic principle and uses air mass trajectories to analyze and calculate the geographical location and spatial distribution of potential source areas. The research region is equally divided into $i \times j$ grid cells, and the ij^{th} cell is determined to affect the pollutant at the research site on the basis of the set pollutant concentration threshold. The PSCF _{ij} value in the ij^{th} cell is calculated by M_{ij}/N_{ij} , and grids with high PSCF _{ij} values are considered potential source regions [35, 44]. The calculation formula of PSCF _{ij} is as follows:

$$\text{PSCF}_{ij} = \frac{M_{ij}}{N_{ij}} \quad (1)$$

where PSCF _{ij} denotes the ratios of M_{ij} and N_{ij} , M_{ij} denotes the number of trajectories that exceed the pollutant concentration threshold passing through the ij^{th} cell, and N_{ij} denotes the total number of trajectories of the air mass passing through the ij^{th} cell. In this study, the resolution of the grid cells was set to $1^\circ \times 1^\circ$, and the seasonal average concentration of PM_{2.5} was set as the threshold.

Uncertainties exist due to the small values of N_{ij} . Therefore, the weight function (W_{ij}) is used to reduce uncertainty [45]. The weight potential source contribution function (WPSCF) is then defined as the PSCF result multiplied by W_{ij} . The calculation formula of W_{ij} is as follows:

$$W_{ij} = \begin{cases} 1 & N_{ij} > 3N_{avg} \\ 0.72 & 1.5N_{avg} < N_{ij} \leq 3N_{avg} \\ 0.4 & N_{avg} < N_{ij} \leq 1.5N_{avg} \\ 0.2 & N_{ij} \leq N_{avg} \end{cases} \quad (2)$$

where N_{avg} denotes the average number of endpoints of the air mass trajectories in the grid cells in the study area.

Enrichment Factor (EF)

The enrichment factor (EF) was used to analyze the relative contributions of anthropogenic sources and natural sources to the metal elements in PM_{2.5} [41, 46]. The calculation formula for the EF is as follows:

$$EF_i = \frac{(C_i/C_{ref})_{PM2.5}}{(C_i/C_{ref})_{soil}} \quad (3)$$

where EF_i denotes the enrichment factor of element i , $(C_i/C_{ref})_{PM2.5}$ denotes the ratio of the concentration of element i to the concentration of the reference element ref in PM_{2.5}, and $(C_i/C_{ref})_{soil}$ denotes the ratio of the concentration of element i to the concentration of the reference element ref in topsoil.

The evaluation criterion of the EFs of elements in PM_{2.5} refers to [41, 47]. When the EF_i of element i is greater than 10, an element is mainly contributed by an anthropogenic source. In contrast, when EF_i is less than 10, the element is contributed mainly by a natural source. The concentrations of the elements in the topsoil were derived from the background values of the topsoil in Sichuan Province [48]. During the sampling period, the average concentration of iron (Fe) at the four sites was lower than that of aluminum (Al), and the concentration of Fe in the PM_{2.5} in the GH was the lowest (Table S2). Therefore, Fe was selected as the reference element, and the Fe in PM_{2.5} at the GH was used to calculate the EFs of the elements in PM_{2.5} at the four sites.

Principal Component Analysis (PCA)

PCA is a multivariate analysis method that can be used as a source apportionment tool to explain the variance in the data effectively and identify the underlying reasons. In this study, the elemental data

Table S2. The background concentrations of topsoil elements in Sichuan Province. The data cited in Background values of soil elements in China (China National Environmental Monitoring Centre, 1990).

Elements	Mean	Unit
Na	0.85	%
Mg	0.85	%
Al	6.26	%
Ca	1.13	%
Fe	3.3	%
K	2.02	%
Mn	657	mg/kg
Cu	31.1	mg/kg
Zn	86.5	mg/kg
As	10.4	mg/kg
Ti	0.4	%
Cd	0.079	mg/kg
Ti	0.4	%
Ni	32.6	mg/kg
V	96	mg/kg
Pb	30.9	mg/kg
Co	17.6	mg/kg
Ba	474	mg/kg
Cr	79	mg/kg

for PM_{2.5} at SQ, GP, JL, and GH during the sampling period were used to quantify the major sources of elements in PM_{2.5} and the contributions of each site via PCA. PCA was performed using SPSS 22.0 statistical software.

Data Processing and Analysis

The PM_{2.5} and element data were analyzed using the statistical software SPSS 22.0. The normality and homoscedasticity of the variables were checked via the Shapiro–Wilk and Levene tests, respectively. Normal and normalizable data were compared via one-way ANOVA (with Duncan's multiple range test). Nonparametric tests (with the Kruskal–Wallis H test) were used when the variables could not be normalized. The values are presented as the means±SEs. Spearman's correlation analysis was used to analyze the correlations between elements.

Origin-pro 9.1 and ArcGIS 10.8 software were used for data processing and graph construction.

Results and Discussion

Overview of PM_{2.5}

During the sampling period, the daily concentrations of PM_{2.5} at SQ ranged from 6.87 to 158.45 µg m⁻³, with 32.58% of daily PM_{2.5} concentrations exceeding the standard. The daily concentrations at GP ranged from 12.48 to 217.54 µg m⁻³, with 22.73% of daily PM_{2.5} concentrations exceeding the standard. The daily concentrations at JL ranged from 12.19 to 191.07 µg m⁻³, with 29.49% of daily PM_{2.5} concentrations exceeding the standard. Finally, the daily concentrations at GH ranged from 8.23 to 210.22 µg m⁻³, with 31.87% of daily PM_{2.5} concentrations exceeding the standard. The upper limit of the daily average PM_{2.5} concentration is 75 µg m⁻³ for Class II areas in the Standard of China's National Air Quality Standard, such as urban residential, commercial and traffic, cultural, industrial, and rural areas) [9]. The average concentrations of PM_{2.5} were 63.03±4.20 µg m⁻³ in SQ, 58.89±4.80 µg m⁻³ in GP, 61.70±4.41 µg m⁻³ in JL, and 60.13±4.28 µg m⁻³ in GH, which were slightly lower than those reported in Chengdu (67.0±43.4 µg m⁻³) and Chongqing (70.9±41.4 µg m⁻³) in the Sichuan Basin [49] but significantly lower than those reported in other cities in China ($P<0.001$), such as Beijing [28-29], Tianjin [28], Shijiazhuang [28], Chengde [28], Shanghai [30], Nanjing [30-31], Hangzhou [30], Ningbo [30], and Wuhan [34-35]. During the study period, the average concentrations at the four sites were significantly greater than that of the Grade II Standard of China's National Air Quality Standard for PM_{2.5} based on a one-sample t test (SQ, $t = 6.682$, $P<0.001$; GP, $t = 4.976$, $P<0.001$; JL, $t = 6.051$, $P<0.001$; GH, $t = 5.865$, $P<0.001$) (the upper limit of the annual average is 35 µg m⁻³ for Class II areas) [9], exceeding the standard by 0.80 times (SQ), 0.68 times (GP), 0.76 times (JL), and 0.72 times (GH). In addition, there was no significant difference in the concentration of PM_{2.5} among the four sites ($\chi^2 = 0.666$, $P = 0.881$), indicating that the PM_{2.5} pollution in the urban and rural areas of Nanchong City was relatively severe during the study period. Lei et al. [50] reported that PM_{2.5} was the major standard-exceeding pollutant in the urban area of Nanchong and that the mean annual concentrations of PM_{2.5} exceeded the Grade II Standard of China's National Air Quality Standard for PM_{2.5} (35 µg m⁻³) from 2015 to 2018. In other cities in the Sichuan Basin, the mean concentrations of PM_{2.5} ranged from 37 µg m⁻³ to 73 µg m⁻³, and the proportion of pollution caused by PM_{2.5} accounted for 77.83% of the total pollution from 2015 to 2016 [51]. These findings indicate that other cities in the Sichuan Basin also suffer from severe PM_{2.5} pollution.

Seasonal Variations in PM_{2.5}

The seasonal variations in the PM_{2.5} concentration at the four sites are depicted in Fig. 2. The concentrations of PM_{2.5} at the four sites were highest in winter, with mean

values of $94.06 \pm 7.07 \mu\text{g m}^{-3}$ in SQ, $94.32 \pm 10.98 \mu\text{g m}^{-3}$ in GP, $90.29 \pm 6.40 \mu\text{g m}^{-3}$ in JL, and $87.25 \pm 6.05 \mu\text{g m}^{-3}$ in GH, followed by spring and fall, with the lowest

concentrations in summer. Compared with those in other seasons, the sources of pollutants in Nanchong City did not change significantly in winter, but the mass

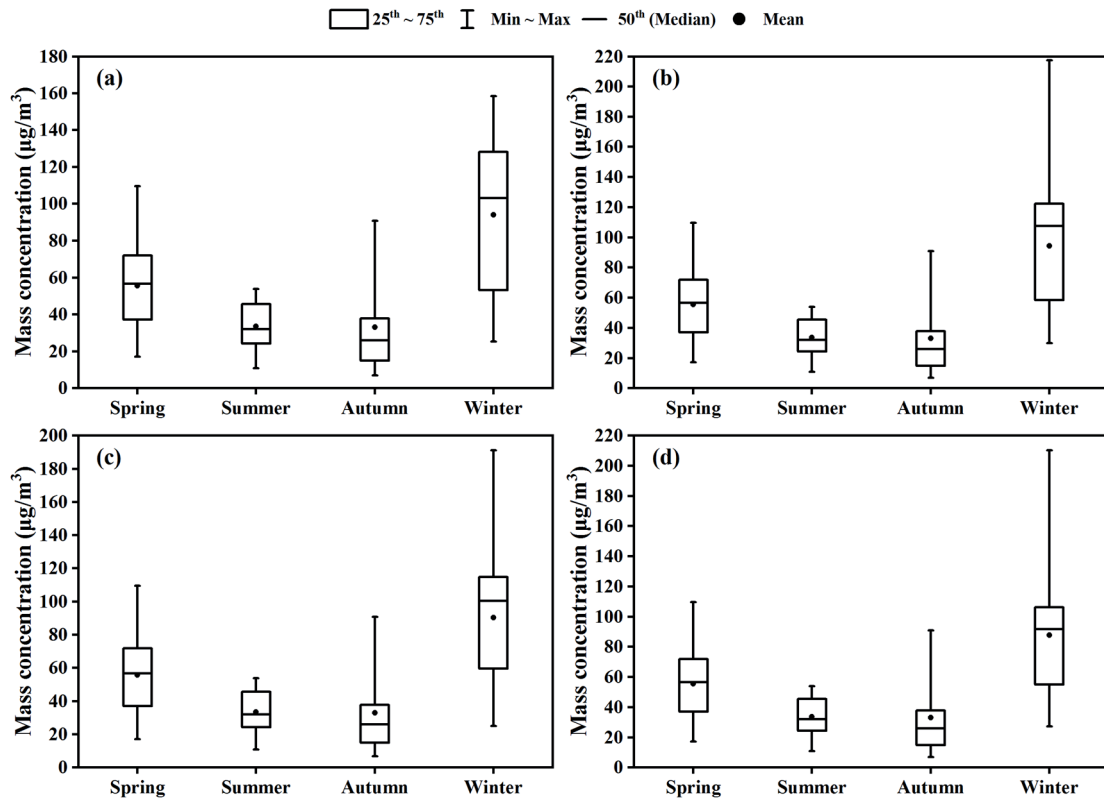


Fig. 2. The seasonal variations of PM_{2.5} concentration in SQ a), GP b), JL c), and GH d).

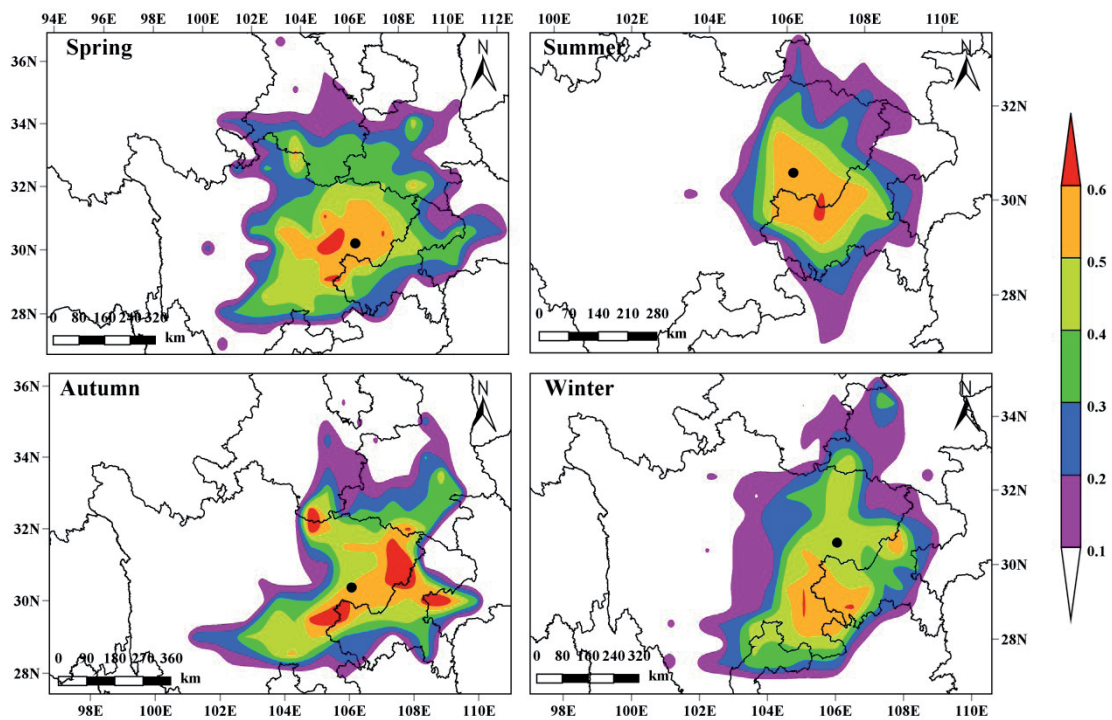


Fig. 3. Seasonal variation of WPSCF values of PM_{2.5} in the urban area of Nanchong City. ●, the location of the urban area of Nanchong City.

concentrations of $PM_{2.5}$ increased significantly (SQ, $\chi^2 = 37.469$, $P < 0.001$; GP, $\chi^2 = 24.025$, $P < 0.001$; JL, $\chi^2 = 38.492$, $P < 0.001$; GH, $\chi^2 = 43.429$, $P < 0.001$). Similar seasonal trends have also been reported in other cities in the Sichuan Basin, such as Chengdu [38, 52-53], Chongqing [49], Leshan [38, 53], Dazhou [38, 53], and Ya'an [53-54]. Studies have shown that the concentration of particulate matter in the urban atmosphere is influenced by source emission intensities [20-21, 49, 55-56], atmospheric processes [49, 57], and meteorological conditions [49-50, 52, 58]. Yang et al. [58] reported that the low-level ventilation volume in cities in the Sichuan Basin is negatively correlated with the $PM_{2.5}$ concentration and that a low wind speed can reduce the diffusion and migration of $PM_{2.5}$, whereas temperature and relative humidity are favorable conditions for secondary aerosol generation.

As shown in Fig. 3, the mass concentration of $PM_{2.5}$ in the urban area of Nanchong City was affected mainly by the surrounding areas because of poor meteorological diffusion conditions for pollutants (such as low wind speeds and high frequencies of calm winds) and advantageous conditions for the generation of $PM_{2.5}$ (such as high temperatures and relative humidity). The proportion of the mass concentration of aerosols in Nanchong from the local and surrounding areas was 79.45% in spring, 85.42% in summer, 83.89% in fall, and 81.12% in winter [41]. In addition, Qiao et al. [59] reported that emissions within the Sichuan Basin contributed approximately 80% of the total $PM_{2.5}$

in Chengdu and Chongqing during the four seasons. Xu et al. [60] also confirmed that $PM_{2.5}$ in Chengdu in winter was less affected by the long-range transport of air masses, and the contribution of the long-traveled air masses was only 12.9%. Although this seasonal trend in $PM_{2.5}$ concentrations has been widely found in cities in northern China [24, 35, 61], the backward trajectories of $PM_{2.5}$ concentrations were completely different from those of cities in the Sichuan Basin, and the contribution of local pollution sources to $PM_{2.5}$ from the end of December 2013 to the end of January 2014 was only 12.9% in Beijing and only 38.7% in Changchun [60]. Local pollution sources contributed no more than 60% of the total $PM_{2.5}$ in Beijing's atmosphere during the whole heating season, and the contribution proportion of local pollution sources was only 40% in the summer [62].

Characteristics of the Elements

Nineteen elements in $PM_{2.5}$ (Na, Mg, Al, Ca, Fe, K, Mn, Cu, Zn, As, Ti, Cd, Se, Ni, V, Pb, Co, Ba, and Cr) were measured in this study. During the sampling period, the total concentrations of the analyzed trace elements at SQ ranged from 0.45 to 20.45 $\mu\text{g m}^{-3}$, with a mean value of $2.81 \pm 0.26 \mu\text{g m}^{-3}$; those at GP ranged from 0.53 to 49.00 $\mu\text{g m}^{-3}$, with a mean value of $3.13 \pm 0.73 \mu\text{g m}^{-3}$; those at JL ranged from 0.41 to 37.36 $\mu\text{g m}^{-3}$, with a mean value of $3.43 \pm 0.62 \mu\text{g m}^{-3}$; and those at GH ranged from 0.15 to 19.02 $\mu\text{g m}^{-3}$, with a

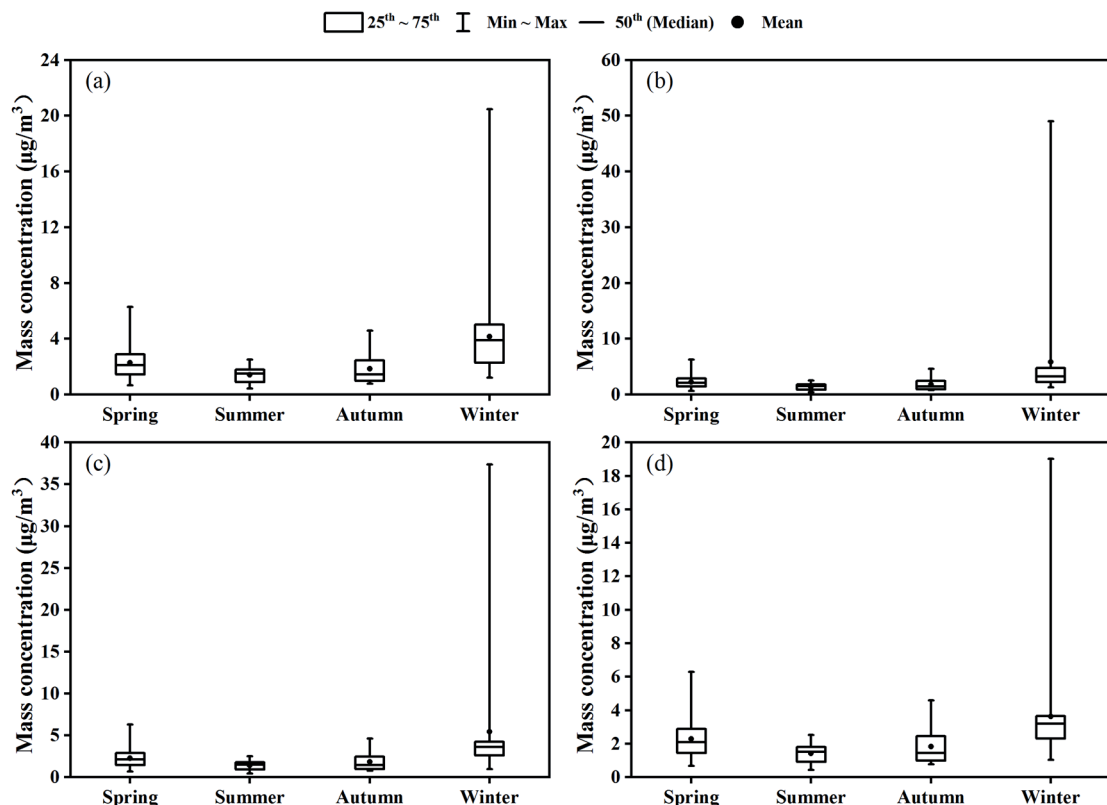


Fig. 4. The seasonal variations of the total concentration of the analyzed trace elements in SQ a), GP b), JL c), and GH d).

mean value of $2.55 \pm 0.26 \mu\text{g m}^{-3}$. These nineteen elements accounted for 1.43%-15.10% of the total mass of $\text{PM}_{2.5}$ in SQ (mean value of $4.84\% \pm 0.25\%$), 1.73%-22.53% of the total mass of $\text{PM}_{2.5}$ in GP (mean value of $4.83\% \pm 0.39\%$), 1.38%-26.33% of the total mass of $\text{PM}_{2.5}$ in JL (mean value of $5.05\% \pm 0.42\%$), and 1.77%-15.73% of the total mass of $\text{PM}_{2.5}$ in GH (mean value of $4.55\% \pm 0.25\%$). The total concentrations of the analyzed trace elements ($\chi^2 = 1.163$, $P = 0.762$) and their mass fractions in $\text{PM}_{2.5}$ ($\chi^2 = 0.816$, $P = 0.846$) did not significantly differ among the four sites. Compared with those in other cities in China, the total concentrations of the analyzed trace elements in the $\text{PM}_{2.5}$ in the urban area of Nanchong City were similar to those in Chengdu [37], Chongqing [37], and Jinan [39] but significantly lower than those in Beijing [28-29], Tianjin [28], Shijiazhuang [28], Chengde [28], Shanghai [30], Hangzhou [30], and Wuhan [34-35] (Table S3). Similarly, the total concentration of elements in $\text{PM}_{2.5}$ in the rural area of Nanchong was lower than that in the suburbs of Beijing [29], Ningbo [30], and Wuhan [29] (Table S3).

Furthermore, there was a significant positive correlation between the total elemental concentration in $\text{PM}_{2.5}$ and the mass fraction of the 19 elements in $\text{PM}_{2.5}$ among the four sites ($P < 0.001$). However, the seasonal differences in the total concentrations of the analyzed trace elements (SQ, $\chi^2 = 31.447$, $P < 0.001$; GP, $\chi^2 = 22.702$, $P < 0.001$; JL, $\chi^2 = 26.281$, $P < 0.001$; GH, $\chi^2 = 38.962$, $P < 0.001$) and the mass fraction of the 19 elements in $\text{PM}_{2.5}$ (SQ, $\chi^2 = 10.099$, $P = 0.018$; GP, $\chi^2 = 9.717$, $P < 0.021$; JL, $\chi^2 = 7.976$, $P < 0.047$; GH, $\chi^2 = 21.846$, $P < 0.001$) at

the four sites reached significant levels. Fig. 4 shows the seasonal variation trends of the analyzed trace elements at the four sites in Nanchong. The seasonal trends of the analyzed trace elements at the four sites were the same as those in $\text{PM}_{2.5}$, with the highest occurring in winter, intermediate values occurring in spring and autumn, and the lowest occurring in summer. However, the seasonal variation trends in the mass fractions of the analyzed trace elements in $\text{PM}_{2.5}$ at the four sites were not the same. The mass fractions of the analyzed trace elements in $\text{PM}_{2.5}$ at sites GP and GH were the highest in autumn, intermediate in spring and winter, and lowest in summer (Fig. 5b and 5d). In contrast to those in GP and GH, the mass fractions of the analyzed trace elements in $\text{PM}_{2.5}$ ranked in the order autumn>summer>winter>spring at site SQ (Fig. 5a) and in the order autumn>winter>summer>spring at site JL (Fig. 5c).

Enrichment Factor (EF)

Fig. 6 shows the mean concentrations of the 19 elements in $\text{PM}_{2.5}$ at the four sites during the sampling period. Generally, the distributions of the 19 elements in $\text{PM}_{2.5}$ were similar among the four sites. K was found to be the dominant element in $\text{PM}_{2.5}$ at the four sites, with K concentrations of $1.24 \pm 0.16 \mu\text{g m}^{-3}$ in SQ (Fig. 6a), $1.51 \pm 0.56 \mu\text{g m}^{-3}$ in GP (Fig. 6b), $1.62 \pm 0.44 \mu\text{g m}^{-3}$ in JL (Fig. 6c), and $1.10 \pm 0.15 \mu\text{g m}^{-3}$ in GH (Fig. 6d). The contribution of K to the total concentration of the analyzed trace elements in $\text{PM}_{2.5}$ was $40.62\% \pm 1.21\%$ in SQ, $38.06\% \pm 1.60\%$ in GP, $38.40\% \pm 1.55\%$ in

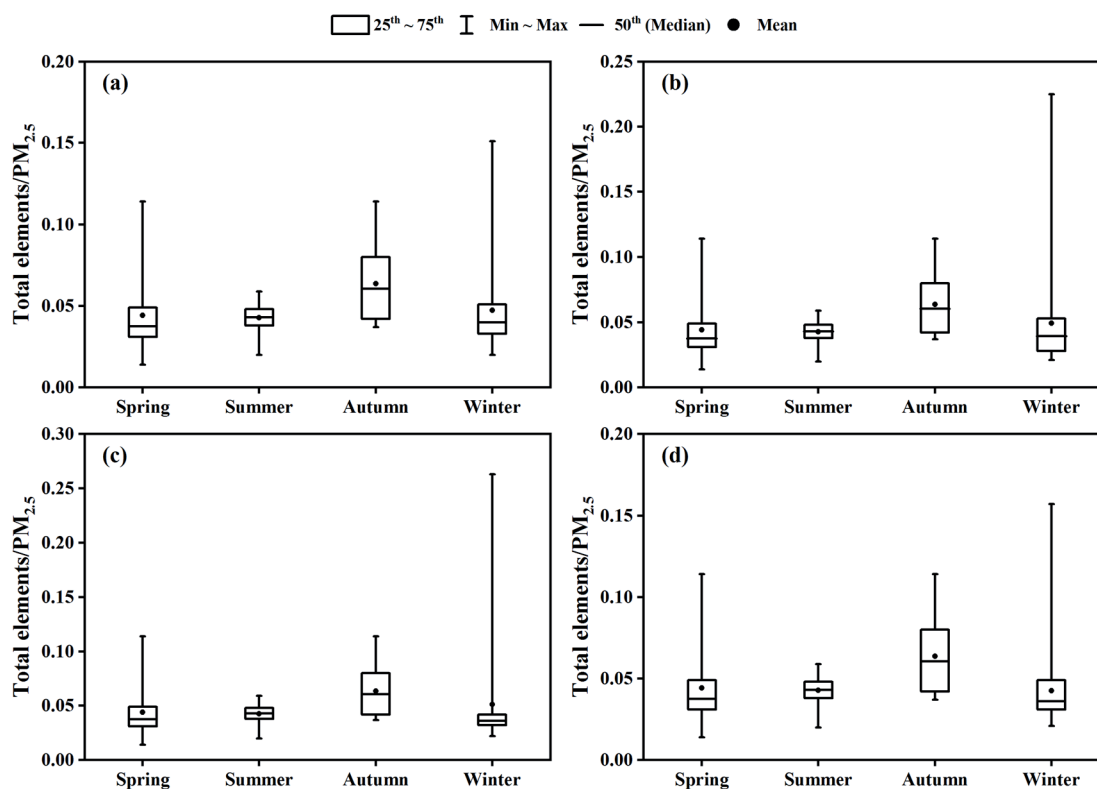


Fig. 5. The seasonal variations of the mass fraction of the analyzed trace elements in $\text{PM}_{2.5}$ in SQ a), in GP b), in JL c), and GH d).

Table S3. The mean concentrations of elements in PM_{2.5} at SQ, GP, JL, GH, and the major cities of China. (unit: ng/m³).

Sampling sites	Sampling site type	K	Ca	Al	Na	Fe	Mg	Zn	Pb	Ba	Ti	Mn	Cu	Cr	Se	V	As	Ni	Cd	Co	Reference
SQ	Urban	1237.51	443.24	315.67	263.33	227.44	124.26	58.09	41.78	30.39	18.28	16.02	12.59	7.00	3.99	2.06	1.84	1.25	1.23	0.16	This study
GP	Urban	1511.05	313.15	462.45	260.48	248.84	126.82	62.08	39.95	35.38	18.29	14.38	9.31	16.68	3.57	2.44	2.20	4.11	1.11	0.18	This study
JL	Urban	1623.54	448.86	472.03	241.46	234.36	173.03	61.39	50.23	54.45	18.43	15.83	14.08	11.17	3.54	1.77	1.94	2.41	1.22	0.17	This study
GH	Rural	1101.91	414.60	390.99	259.81	146.70	88.06	41.48	31.96	21.83	13.99	10.24	10.28	12.64	2.97	2.95	2.80	1.08	1.02	0.12	This study
Chengdu	Urban	720	240	281		456		238	55.4		32.5	33.8	18.7	5.6		1.9	10.8	2.1			(Wang et al., 2018a)
Chongqing	Urban	718	824	429		586		113	50.4		46.5	37.7	11.3	11.1				4.2			(Wang et al., 2018a)
Beijing	Urban	1789.9	641.9	501		1360.9	160.7	291.8	147.1			59.3	49.8	9.5		2.6	10		2.6	0.59	(Li et al., 2019)
Beijing	Suburban	718.6	456.3	383.1		766.6	167.6	180.7	99.9			37.4	23.1	2.0		1.2	9.5		2.0	0.31	(Li et al., 2019)
Beijing	Urban	1730	2420	970		1490	590	320	140	20	40	70	40	20		0	30	10	0	0	(Zhao et al., 2013)
Tianjin	Urban	2150	3280	1170		2020	690	750	220	30	40	100	140	10		0	20	10	0	0	(Zhao et al., 2013)
Shijiazhuang	Urban	3420	4270	1410		1840	640	680	300	40	40	120	40	10		0	20	10	10	0	(Zhao et al., 2013)
Chengde	Urban	1150	1630	750		1280	380	280	110	20	80	60	20	10		10	10	0	0	0	(Zhao et al., 2013)
Shanghai	Urban		1930	922		1340	298	215	69.7				24.2	16.9		16.5		14.9			(Ming et al., 2017)
Nanjing	Urban		1520	705		942	209	247	90.9				24.7	13.2		9.88		9.3			(Ming et al., 2017)
Nanjing	Urban	610	316			577	48.9	199	50.8	13.8	25.9		27.2	6.00	5.15	6.05	11.9	3.62	6.99		(Yu et al., 2019)
Hangzhou	Urban		3020	1370		1720	446	495	122				38.5	17.9		15.3		10.4			(Ming et al., 2017)
Ningbo	Rural		1190	1170		1160	216	190	56.3				16.2	14.6		7.36		8.25			(Ming et al., 2017)
Jinan	Urban	648.7	996.1	647.2	355	655.1	167.9	116.4	64.1	20.3	26.3	29.1	16.8	5.2				0.9	1.9		(Xia et al., 2020)
Wuhan	Urban	3249.17	2043.36			1458.54		388.18	128.79	79.17		50.94	23.26	13.93	8.1	9.01	27.91	3.39		3.51	(Acciai et al., 2017)
Wuhan	Urban	1530	4300			1680	790	290.78	158.4	31.38		97.25	25.27	7.91	6.55		34.71	4.8	4.27		(Zhang et al., 2015)

Wuhan	Suburban	1740	5610	1970	910	350.61	203.00	32.98	82.86	31.45	11.74	7.46	49.37	6.40	5.51	(Zhang et al., 2015)
-------	----------	------	------	------	-----	--------	--------	-------	-------	-------	-------	------	-------	------	------	----------------------

Chengdu: The sampling site (Sichuan Academy of Environmental Science) located in the mixed area of traffic, commerce, residence, and education in Chengdu City, Sichuan Basin of southwest China. The sampling campaign was divided into four periods: autumn (23 October to 18 November, 2014), winter (6 January to 2 February, 2015), spring (2 to 29 April, 2015), and summer (2 to 30 July, 2015).

Chongqing: The sampling site (Chongqing Monitoring Center) located in the mixed area of traffic, commerce, and residence in Chengdu City, Sichuan Basin of southwest China. The sampling campaign was divided into four periods: autumn (23 October to 18 November, 2014), winter (6 January to 2 February, 2015), spring (2 to 29 April, 2015), and summer (2 to 30 July, 2015).

Beijing: The sampling site (Institute of Atmospheric Physics, Chinese Academy of Sciences) located in the mixed area of traffic, residence, and education in Beijing City, China. The sampling period was from September 15 to November 12, 2014.

Beijing: The sampling site (the campus of the University of Chinese Academy of Sciences) located in the suburban area of Beijing City, China. The sampling period was from September 15 to November 12, 2014.

Beijing: The sampling site (local meteorological bureau) located in the mixed area of traffic, commerce, and residence in Beijing City, north China. The sampling campaign was divided into four periods: spring (6 April to 1 May 2009), summer (9 July to 4 August 2009), autumn (11 October to 4 November 2009), and winter (14 January to 8 February 2010).

Tianjin: The sampling site (local meteorological bureau) located in the mixed area of traffic, commerce, and residence in Tianjin City, north China. The sampling campaign was divided into four periods: spring (6 April to 1 May 2009), summer (9 July to 4 August 2009), autumn (11 October to 4 November 2009), and winter (14 January to 8 February 2010).

Shijiazhuang: The sampling site (local meteorological bureau) located in the mixed area of traffic, commerce, and residence in Shijiazhuang City, north China. The sampling campaign was divided into four periods: spring (6 April to 1 May 2009), summer (9 July to 4 August 2009), autumn (11 October to 4 November 2009), and winter (14 January to 8 February 2010).

Chengde: The sampling site (local meteorological bureau) located in the mixed commercial and residential area in Chengde City, north China. The sampling campaign was divided into four periods: spring (6 April to 1 May 2009), summer (9 July to 4 August 2009), autumn (11 October to 4 November 2009), and winter (14 January to 8 February 2010).

Shanghai: The sampling site located in the urban area of Shanghai City, east China. The sampling period was from September 2013 to August 2014.

Nanjing: The sampling site located in the urban area of Nanjing City, east China. The sampling period was from September 2013 to August 2014.

Nanjing: The sampling site (Nanjing Environmental Protection Building) located in the mixed area of traffic, commerce, and residence in Nanjing City, east China. The sampling period was from December 12, 2016 to December 31, 2017.

Hangzhou: The sampling site located in the urban area of Hangzhou City, east China. The sampling period was from September 2013 to August 2014.

Ningbo: The sampling site located in the rural area of Ningbo City, east China. The sampling period was from September 2013 to August 2014.

Jinan: The sampling site (Jinan Environmental Monitoring Center Station) located in the mixed commercial and residential area in Jinan City, East China. The sampling period was from October 1, 2016 to September 30, 2017.

Wuhan: The sampling site (Super Monitoring Station of Wuhan) located in the typical residential urban area of Wuhan city, central China. The sampling period was from May 15 to May 31, 2014.

Wuhan: The sampling site (the campus of the Wuhan University) located in the mixed area of traffic, commerce, residence and education in Wuhan city, central China. The sampling period was from August 2012 to July 2013.

Wuhan: The sampling site (Wuhan East Lake High-tech Zone) located in the suburban area of Wuhan city, central China. The sampling period was from August 2012 to July 2013.

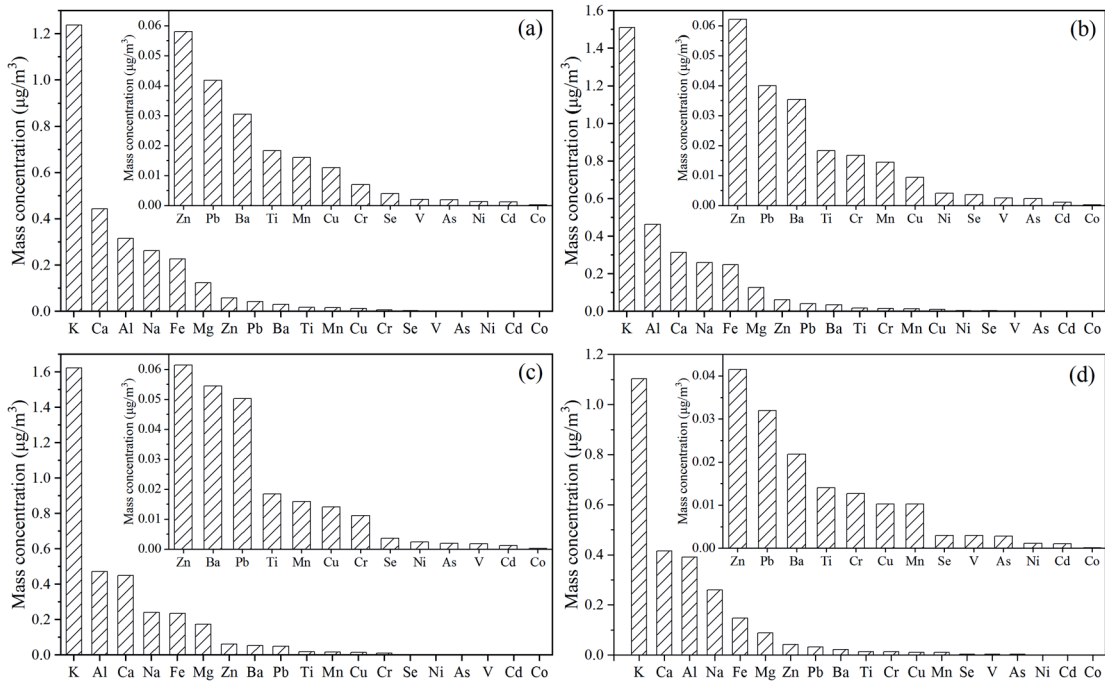


Fig. 6. The mass concentrations of the element in PM_{2.5} in SQ a), in GP b), in JL c), and in GH d).

JL, and 41.73%±1.651% in GH, and there was no significant difference among the four sites ($\chi^2 = 3.812$, $P = 0.283$). The crustal elements K, Ca, Al, Na, Fe, Mg, and Ti were the dominant metals at the four sites, and their contributions to the total concentration of the analyzed trace elements were 93.50%±0.20% in SQ, 93.01%±0.30% in GP, 93.03%±0.26% in JL, and 94.27%±0.21% in GH. Most studies have confirmed that crustal elements are the most important elements in PM_{2.5} and contribute 80.97%-92.73% of the total concentration of the analyzed trace elements in many Chinese cities (Table S3), such as Beijing [28-29], Chengdu [37], Chongqing [37], Tianjin [28], Hangzhou

[30], Jinan [39], Shijiazhuang [28], Ningbo [30], and Chengde [28].

EF analysis has been widely used to determine the source origins (anthropogenic or natural) of elements in PM_{2.5} [38, 47, 63]. K, Ca, Al, Na, Fe, Mg, and Ti were the most abundant elements in PM_{2.5} in Nanchong, and with the exception of the EF of K, which was close to 20, the EFs of the other crustal elements were very low. As shown in Fig. 7, the mean EF of K at the four sites was close to 20, indicating that K was derived mainly from anthropogenic sources. The mean EFs of the crustal elements Mg, Fe, and Al in PM_{2.5} at the four sites were significantly less than 5, indicating that they

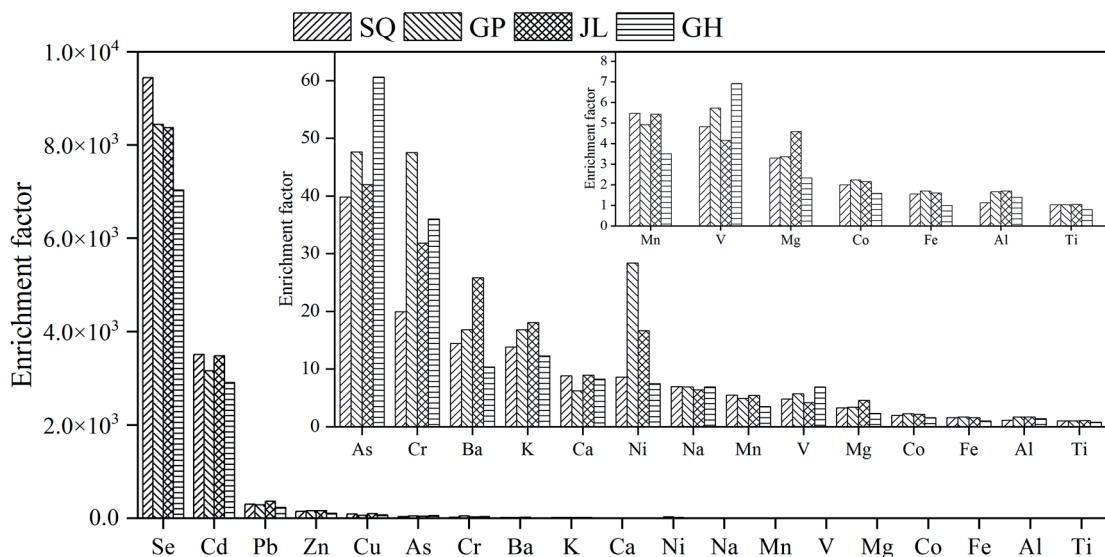


Fig. 7. The element enrichment factors in PM_{2.5} in SQ, GP, JL, and GH.

were derived mainly from natural dust. The mean EFs of the crustal elements Na and Ca and the trace element Ni were close to (or slightly greater than) 10, indicating that they were lightly enriched and influenced by both natural and anthropogenic sources. Unlike crustal elements such as K, Ca, Al, Na, Fe, and Mg, the crustal element Ti and the trace elements Co, V, and Mn have fewer anthropogenic sources, their concentrations were low, and their contributions to the total concentrations of the analyzed trace elements at the four sites were less than 1.10% during the sampling period. Additionally, the EFs of Ti, Co, V, and Mn were less than 10, indicating that they were derived mainly from natural sources (Fig. 7). Nanchong is a typical agricultural city with rapid development and a low level of industrialization. Dust is emitted during the process of urban construction, resulting in a high concentration of crustal elements in $PM_{2.5}$ [50, 64–65]. In addition, owing to the lack of technology for processing straw and the high cost of processing straw, most straw has been burned directly in the past [50], which has contributed to the increase in the concentration of K in $PM_{2.5}$. Yang et al. [65] reported that the contribution rate of biomass burning to OC was greater than 60% in Nanchong City.

In contrast, the remaining 12 elements (Mn, Cu, Zn, As, Cd, Se, Ni, V, Pb, Co, Ba, and Cr) accounted for only 5.73%–6.99% of the total concentration of the analyzed trace elements in Nanchong, and the EFs of Co, V, and Mn were less than 10, suggesting that they were little influenced by anthropogenic sources. However, the EFs of Cu, Zn, As, Cd, Se, Ni, Pb, Ba, and Cr were much greater than 10, suggesting that these elements were mainly contributed by anthropogenic sources.

Source Apportionment via PCA

In this study, the sources of elements in $PM_{2.5}$ were estimated quantitatively via PCA with varimax rotation, and the retention of principal components with eigenvalues greater than 1.0 was used to identify the major pollutant sources. Fig. 8 shows the PCA results for the elements in $PM_{2.5}$ at the four sites.

At the SQ sampling site (the urban site), four principal component factors were found to explain the possible sources of elements in $PM_{2.5}$ (Fig. 8a). Factor 1 (total variance 57.2%) was associated with elements such as Cd, Pb, Cu, K, Mn, and Zn. This group appears to represent a mixture of sources related to vehicular

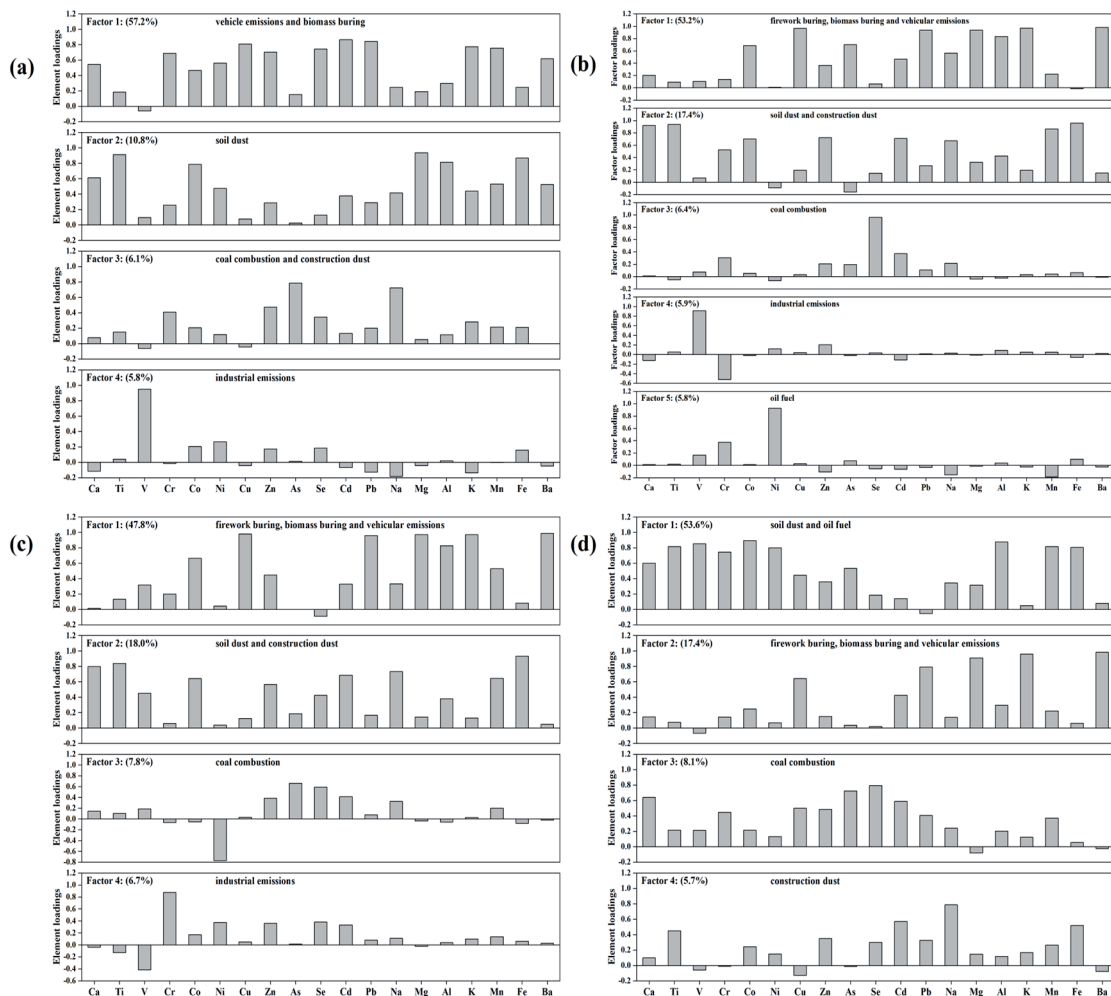


Fig. 8. Varimax-rotated principal component loading for elements in $PM_{2.5}$ in SQ a), in GP b), in JL c), and GH d).

emissions [23, 66-67] and biomass burning [21, 25, 68-69]. Previous studies have shown that Cd is derived mostly from smelting and vehicular emissions [66, 70-71]; Pb and Cu are derived mostly from vehicular emissions [23, 66, 70] and industrial emissions [23, 72]; Zn is derived mostly from vehicular emissions, tire and brake debris, and industrial emissions [66, 73-74]; and Mn is derived from vehicular emissions, coal combustion, metal smelting [67] and soil dust [40, 73]. Cd ($EF_{Cd} = 3513.4$), Pb ($EF_{Pb} = 304.1$), Cu ($EF_{Cu} = 91.1$), Mn ($EF_{Mn} = 5.5$), and Zn ($EF_{Zn} = 151.1$) were significantly enriched and positively correlated with each other at the SQ sampling site ($P < 0.01$), indicating that they were derived mainly from vehicle emissions. Another element with a high degree of loading in factor 1, K, is derived mostly from biomass burning [21, 25, 68-69] and soil dust [40, 73]. The EF of K was 13.8 at the SQ sampling site during the sampling period, which was greater than 10 and much greater than that of other crustal elements (Ca, Al, Na, Fe, Mg, and Ti), indicating that K was strongly influenced by anthropogenic emissions. Therefore, the source of K in factor 1 was mainly biomass burning. The second factor (total variance: 10.8%) was assigned to emissions related to soil dust, a natural source. The crustal elements Mg, Ti, Fe, and Al, which had relatively high loadings in this factor, the EFs less than 5, indicating that they were derived from soil dust [40, 73]. The third factor included As and Na. This factor explains 6.1% of the total variance. It appears to be a mixture of sources related to coal combustion [27, 75-76] and construction dust [27, 77]. Se is frequently used as a marker of coal burning in many studies [75]. Although sodium hydroxide is often used in the exhaust gas desulfurization of coal-fired boilers, the final exhaust gas of coal-fired boilers often contains Na [77]. However, the concentration of Na was significantly greater than that of As at the SQ sampling site during the sampling period ($\chi^2 = 119.853$, $P < 0.001$), and the EF of Na was only 7.0, which was much lower than that of As ($EF_{As} = 39.8$), indicating that Na was less influenced by humans than As. In addition, the EF of Na was close to 10, indicating that Na was affected by certain human activities. Therefore, Na may be derived mainly from construction dust. Factor 4 explains 5.8% of the total variance in the data, with the highest loading of V and high loadings of Co, Se Zn, and Fe, representing contributions from industrial emissions [36].

At the GP sampling site (the urban site), five principal component factors were found to explain the possible sources of elements in $PM_{2.5}$ (Fig. 8b). Factor 1 accounts for 53.2% of the total variance in the data, with Ba, K, Cu, Pb, Mg, and Al exhibiting the highest loadings, representing a mixture of sources related to firework burning [20, 65], biomass burning [21, 25, 68-69] and vehicular emissions [23, 66-67]. The raw materials of fireworks are black powders, and their major components are sulfur, charcoal powder, potassium chlorate, or potassium nitrate. Metal powders containing Cu, Mg, Al, and Ba are used as flame coloring and

glitter additives to add a festive effect. On February 9, 2016, the concentration of Ba was as high as $1.374 \mu\text{g m}^{-3}$, accounting for 0.63% of the total $PM_{2.5}$. In contrast, the concentration of Ba was only 0.015 in the non-Spring Festival period, accounting for only 0.03% of the total $PM_{2.5}$. While the concentrations and proportions of Cu, Mg, and Al were similar to those of Ba, their concentrations and proportions in $PM_{2.5}$ increased significantly during the Spring Festival compared with those during the non-Spring Festival. Factor 2 (17.4%), with high loadings of Fe, Ti, Ca, and Mn, represents soil dust [40, 73] and construction dust [27, 77]. Factor 3, with a high loading of Se, accounts for 6.4% of the total variance and represents coal combustion [27, 75-76]. Factor 4 accounts for 5.9% of the total variance in the data, with V exhibiting the highest loading and Zn and Ni exhibiting relatively high loadings, representing contributions from industrial emissions [36]. Factor 5, explaining 5.8% of the variance and exhibiting the highest loading for Ni and high loadings of Cr and V, is considered related to oil fuel [32-33].

At the JL sampling site (the urban site), four principal component factors were found to explain the possible sources of elements in $PM_{2.5}$ (Fig. 8c). The metal sources at JL are similar to those at GP, and factor 1 accounts for 47.8% of the total variance in the data, with the highest loadings for Ba, Cu, K, Mg, Pb, and Al, representing a mixture of sources related to firework burning [20, 65], biomass burning [21, 25, 68-69] and vehicular emissions [23, 66-67]. Factor 2 (18.0%) is related to soil dust [40, 73] and construction dust [27, 77]. Factor 3 (7.8%) is related to coal combustion [27, 75-76] and is characterized by high loadings of As and Se. Factor 4 (6.7%), with the highest loading of Cr and high loadings of Se, Ni, Zn, and Cd, represents industrial emissions [36].

At the GH sampling site (rural site), four principal component factors were found to explain the possible sources of elements in $PM_{2.5}$ (Fig. 8d). Factor 1 (total variance 53.6%) was assigned to emissions related to soil dust [40, 73] and oil fuel [32-33]. Al, Ti, Mn, and Fe had high loadings in this factor and are indicative of primary crustal sources. V and Ni are considered markers of oil fuel. Factor 2 accounts for 17.4% of the total variance in the data and has high loadings of Ba, K, Mg, and Pb, suggesting that firework burning [20, 65], biomass burning [27, 75-76], and vehicular emissions [27, 75-76] were the major contributors. Factor 3 accounts for 8.1% of the total variance in the data, with high loadings of As and Se representing contributions from coal combustion [27, 75-76]. A high loading of Na is observed in factor 4 (5.7%), which is considered related to construction dust [27, 77].

In general, the metal sources of $PM_{2.5}$ at the urban sampling sites in Nanchong were consistent. Biomass burning, vehicular emissions, firework burning, soil dust, and construction dust were the most important sources of metals in $PM_{2.5}$, and the total contribution of these sources was greater than 65%. Additionally,

the contributions of coal combustion and industrial emissions were relatively low, while contributions from oil fuel were observed only at the GP sampling site. For the rural GH sampling site, the metal sources with the highest contributions to $PM_{2.5}$ were soil dust, oil fuel, firework burning, biomass burning, and vehicular emissions, whereas the contributions of coal combustion and industrial emissions were lower. Nanchong is an agricultural city with a low level of industrial development. Owing to the lack of relevant straw treatment technology and the high cost of straw treatment, many stalks are directly burned in the open air after crop harvest, resulting in a sharp increase in the $PM_{2.5}$ concentration. In addition, Nanchong City is developing rapidly, and it features a large population and a high number of motor vehicles. By the end of 2022, the number of motor vehicles in Nanchong was close to 1.2 million, and the total acreage and population of the main urban area were 171 square kilometers and 1.61 million, respectively. Therefore, vehicular emissions and construction dust are important sources of urban air pollution. In contrast, owing to the lower level of industrialization, the demand for coal in Nanchong has not been high, and since 2000, the main urban area of Nanchong has implemented the policy of replacing coal with gas. Therefore, the contributions of coal combustion and industrial emissions to $PM_{2.5}$ were small.

Conclusions

During the study period, the average concentrations of $PM_{2.5}$ in SQ, GP, JL, and GH were $63.03 \pm 4.20 \mu\text{g m}^{-3}$, $58.89 \pm 4.80 \mu\text{g m}^{-3}$, $61.70 \pm 4.41 \mu\text{g m}^{-3}$, and $60.13 \pm 4.28 \mu\text{g m}^{-3}$, respectively, which exceeded the Grade II Standard of China's National Air Quality Standard for $PM_{2.5}$ by 0.80, 0.68, 0.76, and 0.72 times, respectively. The new Ambient Air Quality Standard (GB 3095-2012) replaced GB 3095-1996 and was implemented in China in 2014, and $PM_{2.5}$ was a newly added monitoring item. During this period, China's economy was in a period of rapid development, and the control of $PM_{2.5}$ in most cities was still in the exploratory stage. As a result, Nanchong, like other cities in China, faces serious $PM_{2.5}$ pollution.

Nanchong City is located in the northeastern Sichuan Basin, it is low in elevation, and the meteorological conditions do not favor pollutant diffusion. Because of these poor meteorological diffusion conditions for pollutant dispersal (such as low wind speeds and high frequencies of calm winds) and advantageous conditions for generating $PM_{2.5}$ (such as higher temperatures and relative humidity), the $PM_{2.5}$ in Nanchong City mainly originates from surrounding areas. There was little difference in $PM_{2.5}$ concentration between the main urban area and the rural areas, and the seasonal trends were the same, with the highest concentration occurring in winter, intermediate values occurring in spring

and autumn, and the lowest concentration occurring in summer.

The total concentrations of the analyzed trace elements in SQ, GP, JL, and GH were $2.81 \pm 0.26 \mu\text{g m}^{-3}$, $3.13 \pm 0.73 \mu\text{g m}^{-3}$, $3.43 \pm 0.62 \mu\text{g m}^{-3}$, and $2.55 \pm 0.26 \mu\text{g m}^{-3}$, respectively, and the mass fractions of those elements in $PM_{2.5}$ were $4.84\% \pm 0.25\%$, $4.83\% \pm 0.39\%$, $5.05\% \pm 0.42\%$, and $4.55\% \pm 0.25\%$, respectively. The total concentrations of the analyzed trace elements and their mass fractions in $PM_{2.5}$ did not significantly differ among the four sites. The seasonal variation trends of the analyzed trace elements at the four sites were consistent, with the highest occurring in winter, intermediate values occurring in spring or autumn, and the lowest occurring in summer. However, the seasonal variation trends of the mass fractions of the 19 elements in $PM_{2.5}$ at the four sites exhibited the highest values in autumn and lowest in spring or summer.

The crustal elements K, Ca, Al, Na, Fe, Mg, and Ti were the most abundant in $PM_{2.5}$ in Nanchong, and their contributions to the total mass of the analyzed trace elements were $93.50\% \pm 0.20\%$, $93.01\% \pm 0.30\%$, $93.03\% \pm 0.26\%$, and $94.27\% \pm 0.21\%$ at the SQ, GP, JL, and GH sites, respectively. The EF of K in Nanchong City was close to 20, indicating that it was mainly contributed by anthropogenic sources, and the EFs of other crustal elements were less than 10, indicating that they were derived primarily from natural sources. In contrast, the remaining 12 elements (Mn, Cu, Zn, As, Cd, Se, Ni, V, Pb, Co, Ba, and Cr) accounted for only 5.73%-6.99% of the total mass of the analyzed trace elements in Nanchong. Nevertheless, the EFs of these elements were each much greater than 50, suggesting that they were contributed mainly by anthropogenic sources.

Nanchong City has a large population, its economy is mainly agricultural, and its industrial development is relatively weak. The PCA results revealed that the $PM_{2.5}$ in the urban area of Nanchong City mainly originates from natural sources such as soil dust and anthropogenic sources such as biomass burning, construction dust, vehicular emissions, and firework burning. In rural areas of Nanchong City, the $PM_{2.5}$ mainly originates from soil dust, oil fuel, biomass burning, firework burning, and vehicular emissions. The contributions of coal combustion and industrial emissions to $PM_{2.5}$ were lower in the urban and rural areas of Nanchong City.

Acknowledgments

The authors sincerely thank Nanchong Ecological and Environmental Monitoring Central Station of Sichuan Province for the permission to access their data. This study was supported by the Science and Technology Plan Project of Nanchong City (22YYJCYJ0001 and 23YYJCYJ0053). The opinions in this study do not reflect the views or policies of Nanchong Ecological and Environmental Monitoring Central Station of Sichuan Province.

Conflict of Interest

The authors declare that they have no conflict of interest.

References

- ZHOU Q., MUHAMMAD N.M., ZHANG H.Y., ZHANG H.L. The air we breathe: An In-depth analysis of PM_{2.5} pollution in 1312 cities from 2000 to 2020. *Environmental Science and Pollution Research*, **30** (41), 93900, **2023**.
- ZHAO Y.Y., ZHANG X.P., CHEN M.X., GAO S.S., LI R.K. Regional variation of urban air quality in China and its dominant factors. *Acta Geographica Sinica*, **76** (11), 2814, **2021** [In Chinese].
- GAUTAM S., PATRA A.K., KUMAR P. Status and chemical characteristics of ambient PM_{2.5} pollutions in China: a review. *Environment, Development and Sustainability*, **21**, 1649, **2019**.
- TAO J., ZHANG L.M., CAO J.J., ZHANG R.J. A review of current knowledge concerning PM_{2.5} chemical composition, aerosol optical properties, and their relationships across China. *Atmospheric Chemistry and Physics*, **17**, 9485, **2017**.
- WANG Y.S., LI W.J., GAO W.K., LIU Z.R., TIAN S.L., SHEN R.R., JI D.S., WANG S., WANG L.L., TANG G.Q., SONG T., CHENG M.T., WANG G.H., GONG Z.Y., HAO J.M., ZHANG Y.H. Trends in particulate matter and its chemical compositions in China from 2013-2017. *Science China (Earth Sciences)*, **62** (12), 1857, **2019**.
- ZHANG X.P., LIN M.H. Comparison between two air quality index systems in study of urban air pollution in China and its socio-economic determinants. *Journal of University of Chinese Academy of Sciences*, **37** (1), 39, **2020**.
- BHATTI U.A., WU G.L., BAZAI S.U., NAWAZ S.A., BARYALAI M., BHATTI M.A., HASNAIN A., NIZAMANI M.M. A pre- to post-COVID-19 change of air quality patterns in Anhui Province using path analysis and regression. *Polish Journal of Environmental Studies*, **31** (5), 4029, **2022**.
- QIN Z., WU J.N. Goal difficulty and effect of air pollution control in major cities of China. *Soft Science*, **36** (8), 72, **2022** [In Chinese].
- MINISTRY OF ENVIRONMENTAL PROTECTION OF THE PEOPLE'S REPUBLIC OF CHINA AND ADMINISTRATION OF QUALITY SUPERVISION AND INSPECTION QUARANTINE OF THE PEOPLE'S REPUBLIC OF CHINA (MEP AND MQSIQ). Ambient air quality standards (GB 3095-2012). Beijing: China Environmental Science Press, **2012** [In Chinese].
- MINISTRY OF ENVIRONMENTAL PROTECTION OF THE PEOPLE'S REPUBLIC OF CHINA (MEP). 2013 report on the state of the environment in China. **2014** [In Chinese].
- MINISTRY OF ECOLOGY AND ENVIRONMENTAL OF THE PEOPLE'S REPUBLIC OF CHINA (MEE). 2022 report on the state of the ecology and environment in China. **2023** [In Chinese].
- XIAO Y.H., HOU L.L., MAO Y.Y. Economic Growth, Urbanization and Air Pollution: An Empirical Study Based on the Yangtze River Delta Urban Agglomeration. *Shanghai Journal of Economics*, **33** (9), 57, **2021** [In Chinese].
- WU R.L., ZHANG Q., ZHAO H.Y., QIN X.Y., LIU S.G., WANG Z., ZHENG Y.X. Source contributions of PM_{2.5}-associated health impacts of 337 cities in China. *Acta Scientiae Circumstantiae*, **43** (11), 173, **2023** [In Chinese].
- XIAO J.Y., HE C., MU H., YANG L., HUANG J.Y., XIN A.X., TU P.Y., HONG S. Spatiotemporal pattern and population exposure risks of air pollution in Chinese urban areas. *Progress in Geography*, **40** (10), 1650, **2021** [In Chinese].
- WU X., LI M., CHEN J., WANG H., XU L., HONG Y., ZHAO G., HU B., ZHANG Y., DAN Y., YU S. The characteristics of air pollution induced by the quasi-stationary front: Formation processes and influencing factors. *Science of the Total Environment*, **707**, 136194, **2020**.
- JIANG S.N., KONG S.F., ZHENG H., ZENG X., CHEN N., QI S.H. Real-time source apportionment of PM_{2.5} and potential geographic origins of each source during winter in Wuhan. *Environmental Science*, **43** (1), 61, **2022** [In Chinese].
- MUSHTAQ Z., SHARMA M., BANGOTRA P., GAUTAM A.S., GAUTAM S. Atmospheric aerosols: some highlights and highlighters, past to recent years. *Aerosol Science and Engineering*, **6**, 135, **2022**.
- BHATTI U.A., ZEESHAN Z., NIZAMANI M.M., BAZAI S. YU Z.Y., YUAN L.W. Assessing the change of ambient air quality patterns in Jiangsu Province of China pre-to post-COVID-19. *Chemosphere*, **288** (2), 132569, **2022**.
- KUMAR R.P., PERUMPULLY S.J., SAMUEL C., GAUTAM S. Exposure and health: A progress update by evaluation and scientometric analysis. *Stochastic Environmental Research and Risk Assessment A*, **37**, 453, **2023**.
- QIAN Y.F., YUAN X., DOU W., HU J., XIA J., LI D.Y., ZHENG Q., ZHANG P., QUAN Q.M., LI Y.X. Effects of fireworks on air quality in the main urban area of Nanchong City during the spring festival of 2014-2019. *Environmental Engineering Research*, **28** (2), 220038, **2023**.
- WANG Z.Y., LI Y.B., GUO L., SONG Z.Q., XU Y.L., WANG F., LIANG W.Q., SHI G.L., FENG Y.C. PM_{2.5} Source apportionment based on a variety of new receptor models. *Environmental Science*, **43** (2), 608, **2022** [In Chinese].
- AHMAD H.R., SIPRA K.M., SARDAR M.F., MAQSOOD M.A., REHMAN M.Z.U., ZHU C.X., LI H.N. Integrated risk assessment of potentially toxic elements and particle pollution in urban road dust of megacity of Pakistan. *Human and Ecological Risk Assessment*, **26** (7), 1080, **2019**.
- DUAN J.C., TAN J.H. Atmospheric heavy metals and Arsenic in China: Situation, sources and control policies. *Atmospheric Environment*, **74**, 93, **2013**.
- TIAN D.Y., FAN J.H., JIN H.B., MAO H.C., GENG D., HOU S.G., ZHANG P., ZHANG Y.F. Characteristic and spatiotemporal variation of air pollution in Northern China based on correlation analysis and clustering analysis of five air pollutants. *Journal of Geophysical Research: Atmosphere-basel*, **125** (8), e2019JD031931, **2020**.
- ZONG Z., WANG X.P., TIAN C.G., CHEN Y.J., QU L., JI L., ZHI G.R., LI J., ZHANG G. Source apportionment of PM_{2.5} at a regional background site in North China using PMF linked with radiocarbon analysis: insight into the contribution of biomass burning. *Atmospheric Chemistry and Physics*, **16** (17), 11249, **2016**.

26. KHAN M.B., SETU S., SULTANA N., GAUTAM S., BEGUM B.A., SALAM M.A., JOLLY Y.N., AKTER S., RAHMAN M.M., SHIL B.C., AFRIN S. Street dust in the largest urban agglomeration: pollution characteristics, source apportionment and health risk assessment of potentially toxic trace elements. *Stochastic Environmental Research and Risk Assessment*, **37** (8), 3305, **2023**.
27. ZHENG M., SALMON L.G., SCHAUER J.J., ZENG L.M., KIANG C.S., ZHANG Y.H., CASS G.R. Seasonal trends in PM_{2.5} source contributions in Beijing, China. *Atmospheric Environment*, **39** (22), 3967, **2005**.
28. ZHAO P.S., DONG F., HE D., ZHAO X.J., ZHANG X.L., ZHANG W.Z., YAO Q., LIU H.Y. Characteristics of concentrations and chemical compositions for PM_{2.5} in the region of Beijing, Tianjin, and Hebei, China. *Atmospheric Chemistry and Physics*, **13**, 4631, **2013**.
29. LI M.L., LIU Z.R., CHEN J., HUANG X.J., LIU J.Y., XIE Y.Z., HU B., XU Z.J., ZHANG Y.X., WANG Y.S. Characteristics and source apportionment of metallic elements in PM_{2.5} at urban and suburban sites in Beijing: implication of emission reduction. *Atmosphere-Basel*, **10** (3), 105, **2019**.
30. MING L.L., JIN L., LI J., FU P.Q., YANG W.Y., LIU D., ZHANG G., WANG Z.F., LI X.D. PM_{2.5} in the Yangtze River Delta, China: Chemical compositions, seasonal variations, and regional pollution events. *Environmental Pollution*, **223**, 200, **2017**.
31. YU Y.Y., HE S.Y., WU X.L., ZHANG C., YAO Y., LIAO H., WANG Q.G., XIE M.J. PM_{2.5} elements at an urban site in Yangtze River Delta, China: High time-resolved measurement and the application in source apportionment. *Environmental Pollution*, **253**, 1089, **2019**.
32. HO K.F., CAO J.J., LEE S.C., CHAN C.K. Source apportionment of PM_{2.5} in urban area of Hong Kong. *Journal Of Hazardous Materials*, **138** (1), 73, **2006**.
33. GUO H., DING A.J., SO K.L., AYOKO G., LI Y.S., HUNG W.T. Receptor modeling of source apportionment of Hong Kong aerosols and the implication of urban and regional contribution. *Atmospheric Environment*, **43** (6), 1159, **2009**.
34. ZHANG F., WANG Z.W., CHENG H.R., LV X.P., GONG W., WANG X.M., ZHANG G. Seasonal variations and chemical characteristics of PM_{2.5} in Wuhan, central China. *Science of the Total Environment*, **518-519**, 97, **2015**.
35. ACCIAI C., ZHANG Z.Y., WANG F.J., ZHONG Z.X., LONATI G. Characteristics and source analysis of trace elements in PM_{2.5} in the urban atmosphere of Wuhan in spring. *Aerosol and Air Quality Research*, **17**, 2224, **2017**.
36. JIANG N., LIU X.H., WANG S.S., YU X., YIN S.S., DUAN S.G., WANG S.B., ZHANG R.Q., LI S.L. Pollution characterization, source identification, and health risks of atmospheric-particle-bound heavy metals in PM₁₀ and PM_{2.5} at multiple sites in an emerging megacity in the central region of China. *Aerosol and Air Quality Research*, **19** (2), 247, **2019**.
37. WANG H.B., QIAO B.Q., ZHANG L.M., YANG F.M., JIANG X. Characteristics and sources of trace elements in PM_{2.5} in two megacities in Sichuan Basin of southwest China. *Environmental Pollution*, **242** (part B), 1577, **2018**.
38. FAN J., SHANG Y.N., ZHANG X.J., WU X.N., ZHANG M., CAO J.Y., LUO B., ZHANG X.L., WANG S.G., LI S.Z., LIU Y.Q., WU P.L. Joint pollution and source apportionment of PM_{2.5} among three different urban environments in Sichuan Basin, China. *Science of the Total Environment*, **714**, 136305, **2020**.
39. XIA Z.Y., HOU L.J., GAO S.L., LI H.B., FU H.X., CHEN Y.J. Pollution characteristics, ecological risk and source analysis of metal elements in PM_{2.5} in Jinan. *Ecology and Environmental Sciences*, **29** (5), 971, **2020** [In Chinese].
40. JIANG N., DONG Z., XU Y.Q., YU F., YIN S.S., ZHANG R.Q., TANG X.Y. Characterization of PM₁₀ and PM_{2.5} source profiles of fugitive dust in Zhengzhou, China. *Aerosol and Air Quality Research*, **18**, 314, **2018**.
41. HU J., XIA J., LI D.Y., LEI X., HE H.J., LI J., TAN S.L., YUAN X., QIAN Y.F. Characteristics and sources analysis of carbonaceous aerosols in urban and rural area of Nanchong city. *Polish Journal of Environmental Studies*, **32** (6), 5599, **2023**.
42. MINISTRY OF ENVIRONMENTAL PROTECTION OF THE PEOPLE'S REPUBLIC OF CHINA (MEP). Technical Guidelines for Source Analysis and Monitoring of Atmospheric Particulates (Trial). **2012** [In Chinese].
43. WANG Y.Q., ZHANG X.Y., DRAXLER R.R. TrajStat: GIS-based software that uses various trajectory statistical analysis methods to identify potential sources from long-term air pollution measurement data. *Environmental Modelling and Software*, **24** (8), 938, **2009**.
44. ASHBAUGH L.L., MALM W.C., SADEH W.Z. A residence time probability analysis of sulfur concentrations at Grand Canyon National Park. *Atmospheric Environment*, **19**, 1263, **1985**.
45. AWANG N.R., RAMLI N.A., YAHAYA A.S., ELBAYOUMI M. Multivariate methods to predict ground level ozone during daytime, nighttime, and critical conversion time in urban areas. *Atmospheric Pollution Research*, **6** (5), 726, **2015**.
46. QIAO B.W., LIU Z.R., HU B., LIU J.Y., PANG N.N., WU F.K., XU Z.J., WANG Y.S. Concentration characteristics and sources of trace metals in PM_{2.5} during wintertime in Beijing. *Environmental Science*, **38**, 34, **2017** [In Chinese].
47. AHMED M., GUO X.X., ZHAO X.M. Spectroscopic and microscopic characterization of atmospheric particulate matter. *Instrumentation Science and Technology*, **45** (6), 659, **2017**.
48. CHINA NATIONAL ENVIRONMENTAL MONITORING CENTRE. Background values of soil elements in China. Beijing: China Environmental Science Press, pp. 259-269, **1990** [In Chinese].
49. WANG H.B., TIAN M., CHEN Y., SHI G.M., LIU Y., YANG F.M., ZHANG L.M., DENG L.Q., YU J.Y., PENG C., CAO X.Y. Seasonal characteristics, formation mechanisms and source origins of PM_{2.5} in two megacities in Sichuan Basin, China. *Atmospheric Chemistry and Physics*, **18** (2), 865, **2018**.
50. LEI X., ZHENG Q., QIAN Y.F., HU J., LI D.Y., ZHANG P., YUAN X., QUAN Q.M., LI Y.X. Feature analysis on air quality in the main urban area of Nanchong City in 2015-2018. *Environmental Engineering Research*, **27** (3), 210006, **2022**.
51. NING G.C., WANG S.G., MA M.J., NI C.J., SHANG Z.W., WANG J.X., LI J.X. Characteristics of air pollution in different zones of Sichuan Basin, China. *Science of the Total Environment*, **612**, 975, **2018**.
52. GUO Q., WU D.Y., YU C.X., WANG T.S., JI M.X., WANG X. Impacts of meteorological parameters on the occurrence of air pollution episodes in the Sichuan basin. *Journal of Environmental Sciences*, **114**, 308, **2022**.
53. FANG C.S., TAN X.D., ZHONG Y., WANG J. Research on the temporal and spatial characteristics of air pollutants in Sichuan Basin. *Atmosphere-Basel*, **12** (11), 1504, **2021**.

54. LI Y.C., SHU M., HO S.S.H., YU J.Z., YUAN Z.B., LIU Z.F., WANG X.X., ZHAO X.Q. Effects of chemical composition of PM_{2.5} on visibility in a semi-rural City of Sichuan Basin. *Aerosol and Air Quality Research*, **29** (1), 957, **2020**.
55. WANG Y., ZHANG H., ZHAI J.X., WU Y.N., CONG L., YAN G.X., ZHANG Z.M. Seasonal variations and chemical characteristics of PM_{2.5} aerosol in the urban green belt of Beijing, China. *Polish Journal of Environmental Studies*, **29** (1), 361, **2020**.
56. CHEN T., ZHOU P., XU W.Q., LIU Y.T., SUN S.W. Spatial-Temporal Evolution Characteristics and influencing factors of PM_{2.5} in the Yangtze River Basin. *Polish Journal of Environmental Studies*, **33** (2), 1611, **2024**.
57. RÖNNKÖ T.J., JALAVA P.I., HAPPO M.S., KASURINEN S., SIPPULA O., LESKINEN A., KOPONEN H., KUUSPALO K., RUUSUNEN J., VÄISÄNEN O., HAO L.Q., RUUSKANEN A., ORASCHE J., FANG D., ZHANG L., LEHTINEN K.E.J., ZHAO Y., GU C., WANG Q.G., JORMA J., KOMPPULA M., HIRVONEN M.R. Emissions and atmospheric processes influence the chemical composition and toxicological properties of urban air particulate matter in Nanjing, China. *Science of the Total Environment*, **639**, 1290, **2018**.
58. YANG Q., XIANG W.G., CHEN Z.H., YANG X.Y. Impacts of low level ventilation and temperature inversion on air quality in Sichuan Basin. *Acta Scientiae Circumstantiae*, **42** (3), 322, **2022** [In Chinese].
59. QIAO X., GUO H., TANG Y., WANG P.F., DENG W.Y., ZHAO X., HU J.L., YING Q., ZHANG H.L. Local and regional contributions to fine particulate matter in the 18 cities of Sichuan Basin, southwestern China. *Atmospheric Chemistry and Physics*, **19** (9), 5791, **2019**.
60. XU H.M., HE K.L., FENG R., SHEN Z.X., CAO J.J., LIU S.X., HO K.F., HUANG R.-J., GUINOT B., WANG Q.Y., ZHOU J.M., SHEN M.X., XIAO S., ZHOU B.H., SONKE J.E. Metallic elements and Pb isotopes in PM_{2.5} in three Chinese typical megacities: spatial distribution and source apportionment. *Environmental Science: Processes and Impacts*, **22** (8), 1718, **2020**.
61. CHENG T., ZHU S.Y., ZHANG G.X., ZHANG H.L., LI J.M. Seasonal variation of PM_{2.5} in the Beijing-Tianjin-Hebei region in 2018 and its relationship with land surface temperature. *Remote Sensing Technology and Application*, **35** (6), 1457, **2020** [In Chinese].
62. LIU X.Y., BAI X.X., TIAN H.Z., WANG K., HUA S.B., LIU H.J., LIU S.H., WU B.B., WU Y.M., LIU W., LUO L.N., WANG Y.X., HAO J.M., LIN S.M., ZHAO S., ZHANG K. Fine particulate matter pollution in North China: Seasonal-spatial variations, source apportionment, sector and regional transport contributions. *Environmental Research*, **184**, 109368, **2020**.
63. JIN X.Y., FAN J.S., NIU H.Y., LING P., YU Q.Q. Analysis of sources and concentrations of heavy metal contents in PM₁₀ over a four-season cycle in a heavily industrialised city in China. *Polish Journal of Environmental Studies*, **28** (5), 3227, **2019**.
64. SHU L., LUO B., HU J., XIA J., ZHANG L., LUO B., ZHONG L.J., ZHANG Z.Q. Emission inventory and characteristics of atmosphere PM_{2.5} and PM₁₀ in Nanchong. *Environmental Monitoring in China*, **34** (3), 84, **2018** [In Chinese].
65. YANG W.W., XIE S.D., ZHANG Z.Q., HU J., ZHANG L.Y., LEI X., ZHONG L.J., HAO Y.F., SHI F.T. Characteristics and sources of carbonaceous aerosol across urban and rural sites in a rapidly urbanized but low-level industrialized city in the Sichuan Basin, China. *Environmental Science And Pollution Research*, **26**, 26646, **2019**.
66. ISLAM M.S., NUR-E-ALAM M., IQBAL M.A., KHAN M.B., AL MAMUN S., MIAH M.Y., RASHEDUZZAMAN M., APPALASAMY S., SALAM M.A. Spatial distribution of heavy metal abundance at distance gradients of roadside agricultural soil from the busiest highway in Bangladesh: A multi-index integration approach. *Environmental Research*, **250**, 118551, **2024**.
67. LIN Y.C., ZHANG Y.L., SONG W.H., YANG X.Y., FAN M.Y. Specific sources of health risks caused by size-resolved PM-bound metals in a typical coal-burning city of northern China during the winter haze event. *Science of the Total Environment*, **734**, 138651, **2020**.
68. LUO J.Q., ZHANG J.K., HUANG X.J., LIU Q., LUO B., ZHANG W., RAO Z.H., YU Y.C. Characteristics, evolution, and regional differences of biomass burning particles in the Sichuan Basin, China. *Journal of Environmental Sciences*, **89** (3), 35, **2020**.
69. ZHU H., DAI L.H., WEI Y., ZHANG Y.J., HU Q.H., WU S.P. Characteristics of inorganic ions and organic components in PM_{2.5} from biomass burning. *Acta Scientiae Circumstantiae*, **37** (12), 4483, **2017** [In Chinese].
70. CHEN H., YAN Y.L., HU D.M., PENG L., WANG C. High contribution of vehicular exhaust and coal combustion to PM_{2.5}-bound Pb pollution in an industrial city in North China: An insight from isotope. *Atmospheric Environment*, **294**, 119503, **2023**.
71. YANG H.H., DHITAL N.B., WANG L.C., HSIEH Y.S., LEE K.T., HSU Y.T., HUANG S.C. Chemical characterization of fine particulate matter in gasoline and diesel vehicle exhaust. *Aerosol and Air Quality Research*, **19** (6), 1439, **2019**.
72. ZHANG Y.P., WANG X.F., CHEN H., YANG X., CHEN J.M., ALLEN J.O. Source apportionment of lead-containing aerosol particles in Shanghai using single particle mass spectrometry. *Chemosphere*, **74** (4), 501, **2009**.
73. LV J.G., LIU S., LI Y.Y. Spatial and seasonal variations of elemental and ion components in air particulate matters in three mega-cities in China. *Environmental Forensics*, **20** (1), 1, **2019**.
74. NAZIR R., SHAH M.H. Evaluation of air quality and health risks associated with trace elements in respirable particulates (PM_{2.5}) from Islamabad, Pakistan. *Environmental Monitoring and Assessment*, **195**, 1182, **2023**.
75. HUANG Y.J., JIN B.S., ZHONG Z.P., XIAO R., TANG Z.Y., REN H.F. Trace elements (Mn, Cr, Pb, Se, Zn, Cd and Hg) in emissions from a pulverized coal boiler. *Fuel Processing Technology*, **86** (1), 23, **2004**.
76. TIAN H.Z., WANG Y., XUE Z.G., CHENG K., QU Y.P., CHAI F.H., HAO J.M. Trend and characteristics of atmospheric emissions of Hg, As and Se from coal combustion in China, 1980-2007. *Atmospheric Chemistry and Physics*, **10** (23), 11905, **2010**.
77. MA Z.H., LIANG Y.P., ZHANG J., ZHANG D.W., SHI A.J., HU J.N., LIN A.G., FENG Y.J., HU Y.Q., LIU B.X. PM_{2.5} profiles of typical sources in Beijing. *Acta Scientiae Circumstantiae*, **35** (12), 4043, **2015** [In Chinese].